School of Mechanical and Manufacturing Engineering

Faculty of Engineering

UNSW Sydney

Biomechanical Modelling of the Left Coronary Artery

Somesh Khullar

5059429

Thesis submitted as a requirement for the degree of Bachelor of Engineering in Mechatronic Engineering

Submitted: Date Student zID: z5059429

Supervisor: Susann Beier (UNSW)

ORIGINALITY STATEMENT

'I, Somesh Khullar hereby declare that this submission is my own work and to the best of my knowledge it contains no materials previously published or written by another person, or substantial proportions of material which have been accepted for the award of any other degree or diploma at UNSW or any other educational institution, except where due acknowledgement is made in the thesis. Any contribution made to the research by others, with whom I have worked at UNSW or elsewhere, is explicitly acknowledged in the thesis.

I also declare that the intellectual content of this thesis is the product of my own work, except to the extent that assistance from others in the project's design and conception or in style, presentation and linguistic expression is acknowledged.'

Signed

Date 2020-05-12

Abstract

Research Question: Investigate the impact of including FSI effects when employing biomechanical models to estimate WSS and TAWSS in the left coronary artery relative to the cost of model implementation.

Findings: The inclusion of FSI effects lead to meaningful difference on solving time but not on WSS and TAWSS measurement with neglible impact of changes in linear elastic material stiffness on findings.

Limtations and Future Work: To verify findings in more realistic models, future work should investigate how patient derived geometries and nonlinear elastic structural models can influence findings using an explicit dynamic solver to reduce data obtainment problems.

Acknowledgements

Work on this project would not have been possible without the direct and indirect support of many beings and I would like to express my gratitude to all them for this, with particular thanks to:

My supervisor Dr Susann Beier, whom gave me the opportunity to work on this insightful project that has helped shaped both my professional and personal development.

Research Technology Services at UNSW Sydney, whom facilitated access and maintaince of the computational cluster Katana which was employed for running the biomechanical models employed for this project.

Ramtin Gharleghi, whom provided much support with managing problems with employing computational resources.

Dr Harkamaljot Kandail, for providing their expertise with developing the Fluid Structure Interaction Simulations.

Heidi Wright and Eranda Dissanayake, for all their helpful assistance and and warm banter.

And to my friends and family for providing all their support throughout the duration of this project.

Table of Contents

Abstract iii
Acknowledgements iv
List of figures vi
List of tables vi
Nomenclature vii
1. Introduction 1
1.1 Coronary Artery Disease 2
1.2 Biomechanical Data 2
1.2.1 Utility of Biomechanical Data 2
1.2.2 Methods for Obtaining Biomechanical Data 3
1.3 Numerical Modelling 4
1.3.1 Overview of Numerical Modelling 4
1.3.2 Computational Fluid Dynamics 4
1.3.3 Fluid Structure Interaction 5
2. Literature review 6
2.1.1 Findings 9
3. Gap In Research and Aim 11
4. Methodology 12
4.1 Modelling 12
4.2 Implementation 16
4.3 Workflow Development and Barriers 17
5. Results and discussion 18
5.1 Material Models 18
5.1.1 WSS Comparison 18
5.1.2 TAWSS Comparison 21
5.1.3 Solving Time Comparison 24
5.1.4 Verification and Validation 25
5.2 Limitations and Future Recommendations 26
6 Conclusions 26
References 27

List of figures

Figure 1: Aims and Context of Current Research 1
Figure 2: Overiview of Coronary Arteries, wih figure adapted from [7], [8],[9] 3
Figure 3:Coronary Artery Material Response adapated from[22] 6
Figure 4: Nonlinear Elastic Material Models, image obtained from [23] 7
Figure 5:Idealised Geometry Model and Mesh Settings 12
Figure 6: Material Model Comparision Graph 15
Figure 7: Rigid Wall Simulation Workflow Setup 16
Figure 8: FSI Simulation Workflow Setup 16
Figure 9: Comparison between Rigid Wall vs L700k model shown as contour plot(below), and as a graph depicting WSS in the ROI(top left) and the difference in WSS between model in the ROI(top right) 18
Figure 10:Comparison between Rigid Wall vs L1500k model shown as contour plot(below), and as a graph depicting WSS in the ROI(top left) and the difference in WSS between model in the ROI(top right) 19
Figure 11: Comparison of WSS contour plots between L700k and 1500k models(above) and WSS between 3 models within ROI 20
Figure 12: Comparison between Rigid Wall vs L700k model shown as contour plot(below), and as a graph depicting TAWSS in the ROI(top left) and the difference in TAWSS between model in the ROI(top right) 21
Figure 13: Comparison between Rigid Wall vs L1500k model shown as contour plot(below), and as a graph depicting TAWSS in the ROI(top left) and the difference in TAWSS between model in the ROI(top right) 22
Figure 14:TAWSS Comparision between L700k and 1500k models 23
Figure 15: Solving Time Comparision 24

List of tables

Table 1: Coronary Artery Material Response 6
Table 2:FSI Numerical Methods 8
Table 3:Overview of Select FSI Based Studies 10
Table 4:Nonlinear FSI simulation debugging tests 17
Table 5: Mesh Verifcation Test 25

Nomenclature

CFD = Computational Fluid Dynamics

E = Young's Modulus (units kPa)

FSI = Fluid Structure Interaction

IBV = Idealized Bifurcated Vessel

ISV = Idealized Single Vessel

L700k = Linear Elastic Material Model with Young Modulus of 700kPa

L1500k = Linear Elastic Material Model with Young Modulus of 1500kPa

MR2 = Mooney Rivlin 2 Parameter Model

MR5 = Mooney Rivlin 5 Parameter Model

PBV = Patient-Specific Bifurcated Vessel

PSV = Patient-Specific single Vessel

ROI = Region of Interest

RW = Rigid Wall

WSS = Wall Shear Stress

TAWSS = Time Averaged Wall Shear Stress

1. Introduction

-

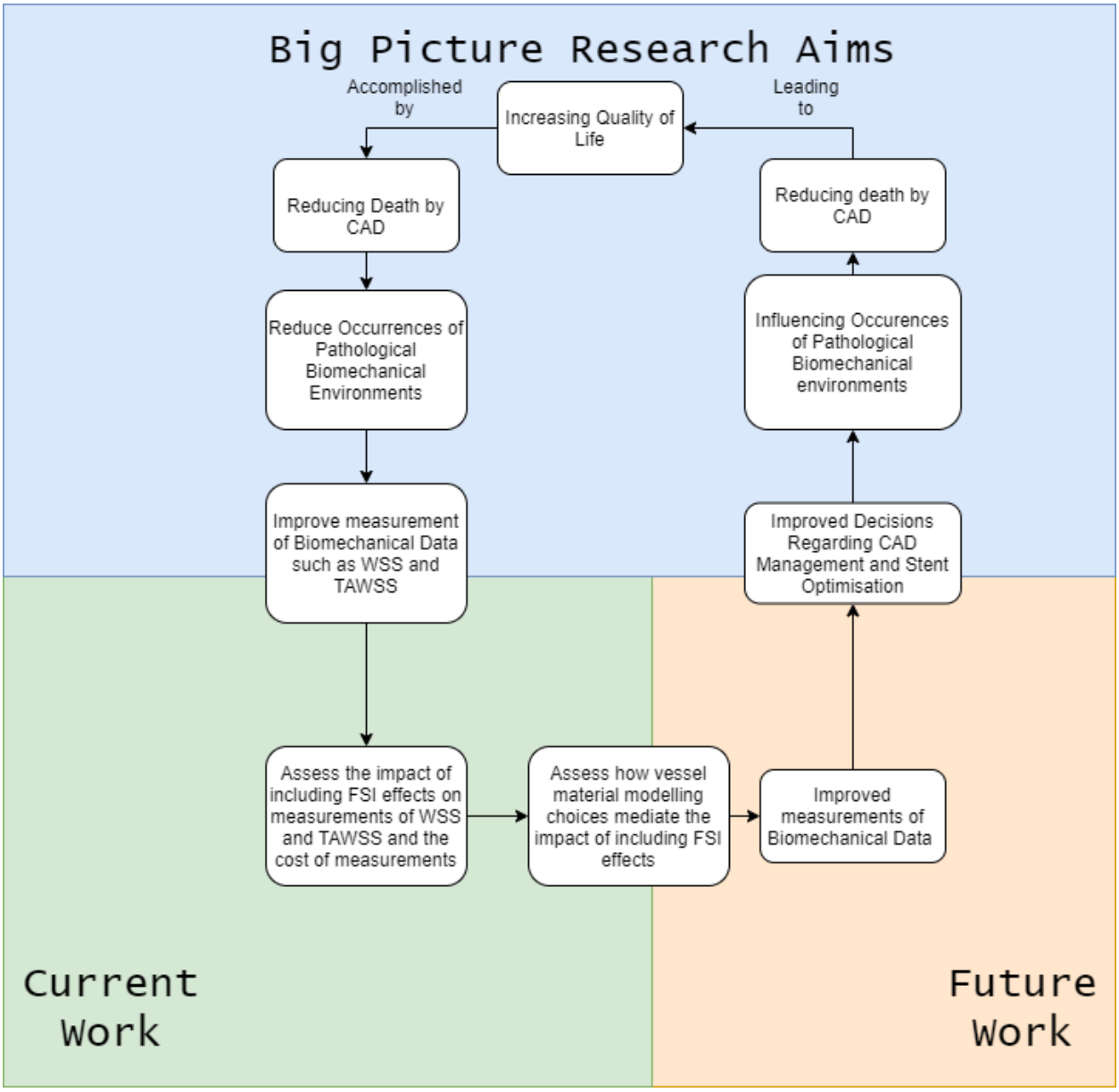

Figure 1: Aims and Context of Current Research

1.1 Coronary Artery Disease

Coronary Artery Disease (CAD), is a condition where heart tissue perfusion becomes obstructed as result of the progressive pathological build up and potential detachment of a biochemical mixture, plaque; within the coronary artery walls [1]. Those with this condition may experience changes in their lifestyle and lifespan, with a significant portion of human deaths associated with CAD [2].

Treatment

Coronary artery stents have been developed to manage the effects of CAD, by providing a scaffold to counteract obstructions to blood flow. Unfortunately, a subset of patients provided with stents may experience clinical complications in the form of in-stent restenosis(ISR) and in-stent thrombosis (IST), which could result in the re-obstruction of cardiac tissue perfusion, leading to worsening in patient outcomes [3].

1.2 Biomechanical Data

1.2.1 Utility of Biomechanical Data

The occurrence of these complications have been partially attributed to the biomechanical environment within coronary artery lumen(Figure 2. Whilst blood pressure has been commonly associated with cardiovascular disease other mechanical stimuli have been associated with CAD progression through their potentially ability to activate pathological biochemical reactions in the endothelial cells that line the lumen[4]. A key method for quantifying a subset of these stimuli is through the following metrics:

Wall Shear Stress (WSS)

$$|WSS| = |\eta_i \tau_{ij}|$$

η_i - surface normal vector

τ_{ij}- viscous stress tensor

- Low WSS is proposed to facilitate ISR [4]
- High WSS linked to IST occurrence [5]

Time Averaged Wall Shear Stress (TAWSS) - WSS averaged against cardiac cycle time. [6]

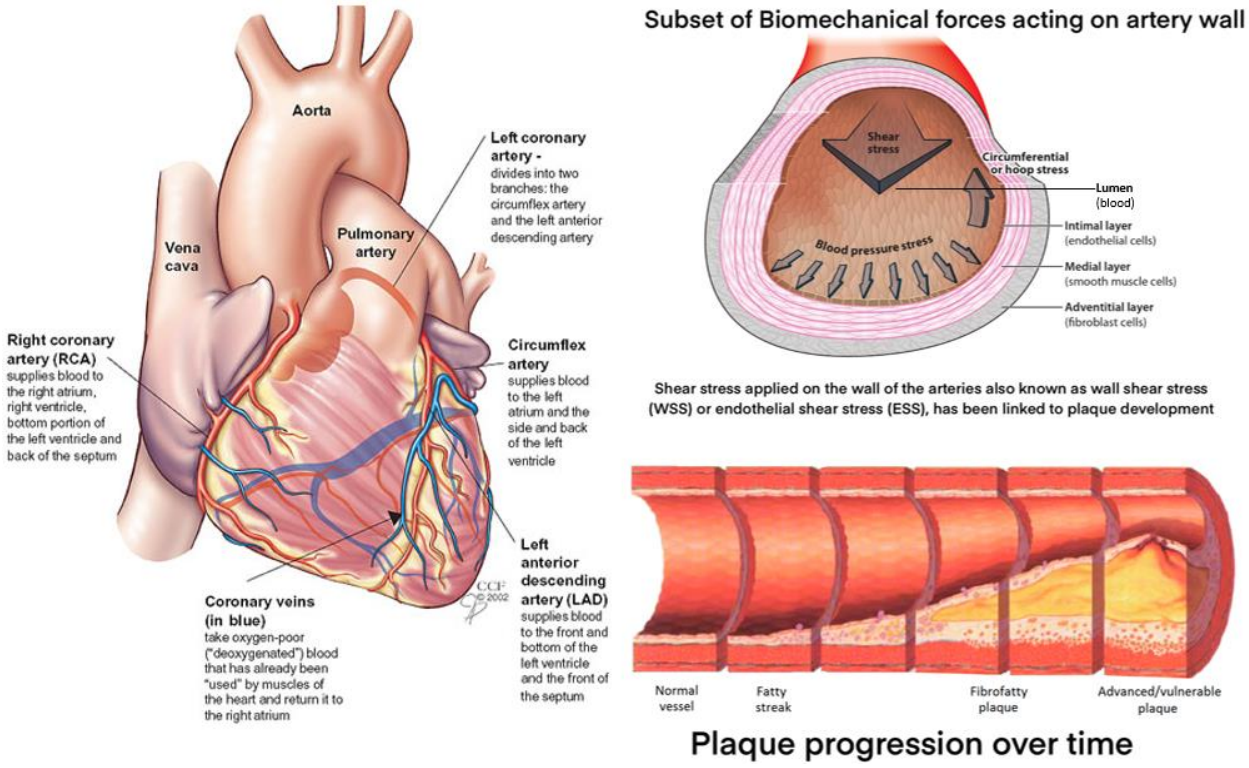

Figure 2: Overiview of Coronary Arteries, wih figure adapted from [7], [8],[9]

1.2.2 Methods for Obtaining Biomechanical Data

These metrics provide a foundation from which assessments can be made of the biomechanical environment within the coronary arteries. The data obtained from such assessments may facilitate improvements in CAD management[1], particularly through facilitating threshold analysis to enable stent design optimisation, which may lead to reduction in ISR and IST occurrence [10].

Obtaining this data through in vitro methodology represent an active area of research with recommendations provided for future research to incorporate vessel compliance as part of in-vitro models through implementation of linear elastic isotropic material properties[11]. However limitations with data resolution of this approach has lead to an alternate methodology as being preferred for obtaining this data, that involving computational/numerical modelling [12]

1.3 Numerical Modelling

1.3.1 Overview of Numerical Modelling

Numerical modelling has emerged as methodology for obtaining this data at minimal patient risk compared to direct patient measurements[13] .

Numerical modelling refers to the process of making simplifications regarding the behaviour of interest to define a quantitative model that can then be solved with the aid of computers to obtain the data of interest. Information gained from this quantitative model can then be interpreted with respective to the original problem to gain useful insights.

1.3.2 Computational Fluid Dynamics

A common implementation of this method when studying the coronary arteries, is to model the biomechanical environment within the artery lumen as being only influenced by blood flow modelled as continuum(responses of individual red blood cells are ignored), with the behaviour of blood governed by the Navier-Stokes(N-S) equations. Further simplifications are made to simplify blood movement as being laminar and not influenced by heat transfer.The solutions to the simplified equations are then obtained with the aid of computers through numerical techniques to obtain approximate solutions from which the desired data could be obtained. The two main approach for this include: Finite Volume Method and Finite Difference Method.

This particular implementation of Numerical Modelling is referred to Computational Fluid Dynamics (CFD) [14], [15].

Whilst significant research has been conducted by applying the CFD methodology [16], [17], many studies have noted the need for future models to incorporate the compliant nature of the coronary artery walls, to obtain more realistic data [18]–[20].

1.3.3 Fluid Structure Interaction

This could be possible through a Fluid-Structuration Interaction (FSI) methodology. This refers to a numerical modelling technique in which the interacting effects of fluid motion and structural deformation are incorporated as part of the equations solved to obtain the desired data [1], [14].

To accomplish this, two major research developments have been needed (Zhong et al., 2018).

- Development of models to approximate material behaviour of the coronary arteries
- Advancement in numerical modelling techniques to incorporate the interaction effects of between fluid and a structure.

2. Literature review

Arteries and Constitutive Modelling

Experimental tests conducted on the human coronary arteries(example data shown in the figure below), ave found them to have a material response that can be described as:

Table 1: Coronary Artery Material Response

Anisotropic	Direction of stress application can influence the material response. This is attributed to the presence and direction of collagen fibres within the artery walls[13]
Hyperelastic/ Nonlinear	The complete stress strain response within an elastic response range, cannot be completely represented by a linear(straight line) material response model [13]
Heterogenous	The material response of the arteries can vary based on multiple patient specific factors such as age and sex.[21]

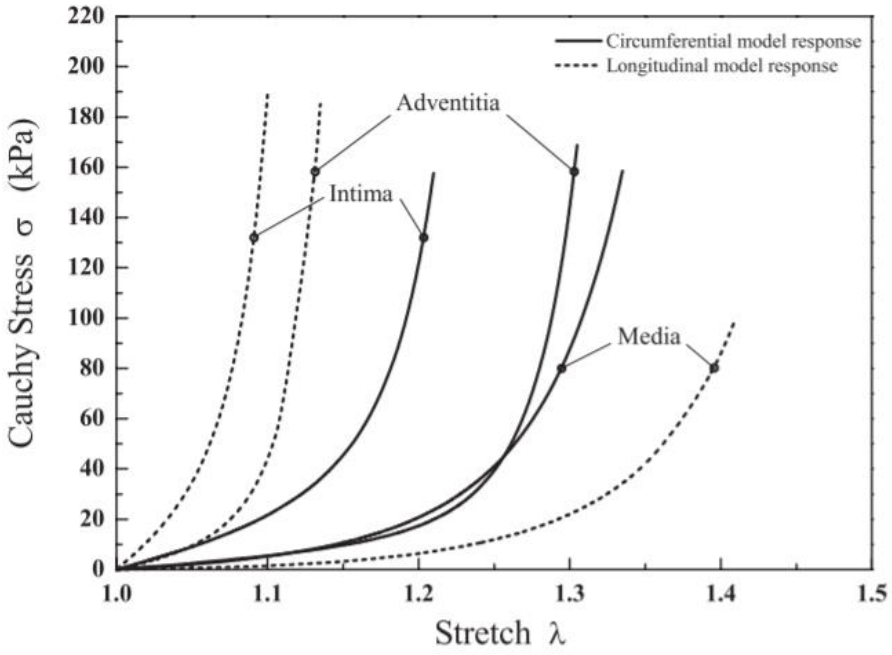

Figure 3:Coronary Artery Material Response adapated from[22]

To approximate the artery material response various constitutive models have been employed alongside the common linear elastic model with common models shown in the figure below

Nonlinear strain-energy functions for characterizing the biomechanical response of arterial tissues used in FE studies as displayed in Table 1 (I_1, I_2, I_4, I_6=invariants; c_1, c_2, c_{10}, c_{01}, c_{20}, c_{11}, c_{02}, μ_p, α_p, a, b, k_1, k_2, ρ=material parameters; λ_1, λ_2, λ_3=principal stretches; κ=dispersion parameter; α_p, b, k_2, ρ and κ are dimensionless parameters while the remaining are stress-like material parameter).

	Strain-energy function
Neo-Hookean model	$\Psi = c_1(I_1-3)$
Mooney–Rivlin model	$\Psi = c_1(I_1-3)+c_2(I_2-3)$
5-Parameter Mooney–Rivlin model	$\Psi = c_{10}(I_1-3)+c_{01}(I_2-3)+c_{20}(I_1-3)^2 + c_{11}(I_1-3)(I_2-3)+c_{02}(I_2-3)^2$
Ogden (1972)	$\Psi = \sum_{p=1}^{N} \frac{\mu_p}{\alpha_p}(\lambda_1^{\alpha_p}+\lambda_2^{\alpha_p}+\lambda_3^{\alpha_p}-3)$
Demiray (1972)	$\Psi = \frac{a}{b}\left\{\exp\left[\frac{b}{2}(I_1-3)\right]-1\right\}$
Holzapfel et al. (2000)	$\Psi = c_1(I_1-3)+\frac{k_1}{2k_{2i=4,6}}\sum\left\{\exp[k_2(I_i-1)^2]-1\right\}$
Holzapfel et al. (2005a)	$\Psi = c_1(I_1-3)+\frac{k_1}{2k_{2i=4,6}}\sum[\exp\{k_2[(1-\rho)(I_1-3)^2] + \rho(I_i-1)^2]\}-1]$
Gasser et al. (2006)	$\Psi = c_1(I_1-3)+\frac{k_1}{2k_{2i=4,6}}\sum\left\{\exp[k_2(I_i^*-1)^2]-1\right\}$ $I_i^* = \kappa I_1+(1-3\kappa)I_i$

Figure 4: Nonlinear Elastic Material Models, image obtained from [23]

FSI and Numerical Techniques

Two main numerical methods have been developed to facilitate numerical modelling of fluid structure interaction

Table 2:FSI Numerical Methods

Arbitrary Euler Lagrange (ALE) Method	A commonly implemented method that is considered that gold standard when developing FSI simulation[23]that generates incorporates interaction effects with a model through an interface that allows for transfer of fluid forces and structural deformation. The structural deformation information is transferred through the fluid domain to facilitate changes in the fluid domain discretization(mesh). This process continues iteratively for each time step until desired numerical convergence criteria is meet. A key disadvantage of this method is the high computational cost associated with it [1].
Immersed Boundary Method (IBM)	A less commonly applied method, that whilst being computation cheaper to implement compared to ALE method, still needs to be developed to account for interaction effects from large structural deformation [1].

2.1.1 Findings

Whilst many FSI based studies have been conducted(subset shown in Table 3) it is noted that the influence of artery compliance on haemodynamic data obtained from FSI studies, was found to be both significant [24] and negligible[25] compared to treating the vessel wall as a rigid structure.

These results can lead to confusion regarding the necessity of obtaining data through FSI vs CFD approach, with the importance of justifying this choice necessary considering the added costs associated with conducting the former relative to the latter [26]. For certain industrial and academic research such costs may be infeasible to serve, thus limiting the utility of the FSI methodology.

It is proposed that the discrepancies in these studies could be the result of difference in constitutive model employed.

Table 3:Overview of Select FSI Based Studies

Author	Geometry	Material Modelling Choices	Difference Observed between Data obtained from different material models	Differences Observed between cost of data obtained
Chiastra et al. [25]	ISV + Stent	hyperelastic isotropic incompressible homogeneous material Rigid Wall	Non Significant difference observed	FSI simulation took more than 100hr
Dong et al. [24]	IBV & PBV	hyperelastic nine parameter Mooney–Rivlin homogeneous material Rigid Wall	Significant difference observed	Course Mesh: 398K elements -13h Fine Mesh : 819K - 21h Finest Mesh - 1.977M - 35
Malvè et al. (2012) [27]	IBV	hyperelastic incompressible isotropic and homogeneous material	the minimum and maximum WSS values significantly vary	not reported
Meza et al. 2018 [28]	PSV	hyperelastic, anisotropic, nearly-incompressible and homogeneous material using a modified hyper-elastic Mooney–Rivlin model	a significant effect on local hemodynamics and vascular wall stress/strain distribution. increased blood flow velocity and fluid wall shear stress, but also changed shear stress patterns.	not reported
Wang et al. 2018 [29]	PSV	Mooney–Rivlin model	not compared	not reported
Wu et al. (2015) [30]	ISV + Stenosis	isotropic nearly incompressible material with E = 5 MPa	not compared	not reported
Wang et al. [31]	PSV + Plaque	isotropic nearly incompressible material with E = 0.6 MPa	significant difference observed	not reported
Eslami et al. [23]	PBV	isotropic nearly incompressible material with E = 0.1 MPa and 1MPa	slight difference in WSS but neglible difference in TAWSS	not reported

3. Gap In Research and Aim

Gaps in Research

Based on this review the following gaps in the literature were observed:

- More data is needed regarding the utility of including FSI effects when obtaining WSS and TAWSS to help clarify discrepant findings in the literature
- Assess whether vessel material modelling choices are influencing these findings

Aim:

As a first step, towards filling these gap, this project aimed

- to investigate the impact of including FSI effects when obtaining WSS and TAWSS measurements in a biomechcanical model of an idealized coronary artery
- Observe how material modelling choices could alter the impact of including FSI effects by comparing WSS, TAWSS and Solving Time obtained from
    - Rigid Wall – to represent the modelling without including FSI effects as done using
    - Linear Elastic Isotrpoic with E=700kPa(L700k) [11] – simplest FSI model to approximate a portion of coronary artery material behaviour
    - Linear Elastic Isotropic with E=1500kPa(L1500k) [11] – to approximate a different portion of coronary artey material behaviour as well generate data that could support in vitro work on WSS measurements
    - Nonlinear Elastic Isotropic - Mooney Rivlin 2 Parameter(MR2) – to assess the effect of a model that may better approximate the nonlinear coronary artery material behaviour
    - Nonlinear Elastic Isotropic - Mooney Rivlin 5 Parameter(MR5) – to assess the effect of a commonly employed FSI model that has been shown to approximate experimental data better than the previous four models

4. Methodology

4.1 Modelling

To develop the model the following set of assumption were made

Geometric Assumptions

To approximate the coroonary artery geometry for this project the left coronary arteries were approximated approximated as a idealised single vessel geometry with a:

- Diameter of 3mm
- Length of 12mm
- Vessel Wall Thickness - 0.435mm uniform through the vessel Fluid Modelling[22]

With hexahedral mesh employed to discretise the fluid and structutral geometry

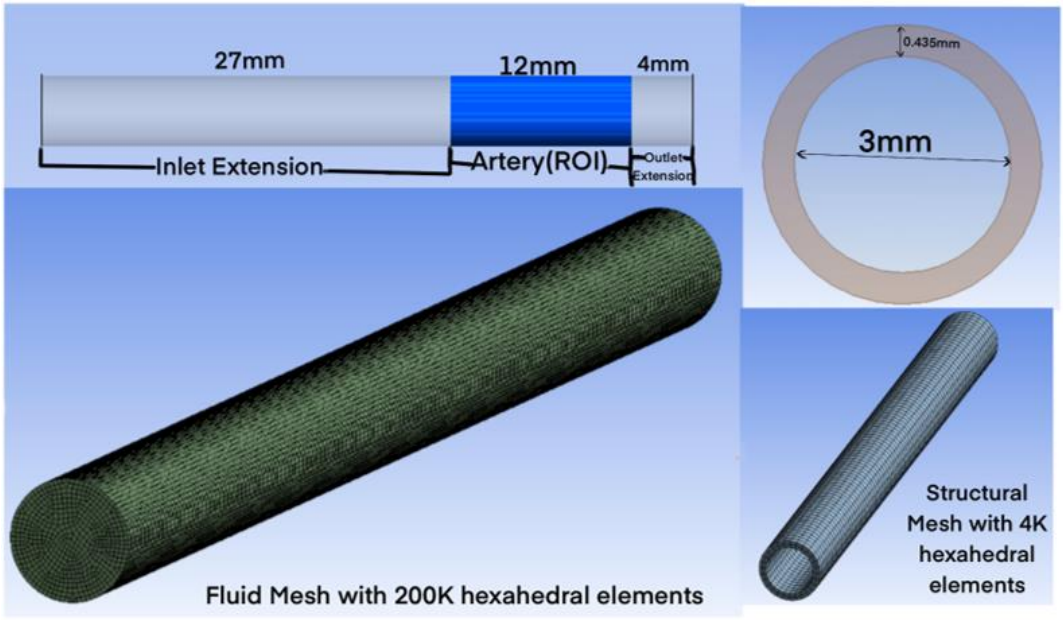

Figure 5:Idealised Geometry Model and Mesh Settings

Blood Behaviour Assumption

Blood behaviour was approximated using the workflow from previous study employing biomechanical modelling in the context of stent optimization[10]The material response of blood was approximate as non-newtonian fluid using the Carreau Yasedua with blood density =1050kg/m^3

Blood motion was approximated as laminar,incompressible with no heat transfer and governed by the Navier Stokes Equation, with pulsatile inlet and static pressure outlet.

To ensure fully developed flow conditions inlet and outlet extensions (27mm and 4mm respectively were employed)

The simulations would run using timesteps of 0.008s for 2.88s to simulate 4 cardiac cycles would the results from the last cardiac cycle employed to reduce result contamination through startup effects. In particular results would be analysed at time of peak flow (t=2.72s) as it was believed that the greatest differences would be observed here

Vessel Wall Behaviour Assumption

To assess the effect of material modelling choices on the impact of including FSI effect the artery wall material response was planned to be modelling using all of the material models shown below in order of best fit to experimental data shown in Figure 4

- Rigid Wall (no deformation)
- Deformable Wall with Density = 1160 kg/m^3, with one of the following material model
    - Linear Elastic Isotropic Material with poisson ratio =0.48 and
        - E= 700k
        - E= 1500k
    - Nonlinear Elastic Isotropic Model with parameter values found by fitting material data from uniaxial testing of the coronary initima in the longitudinal direction[22]
        - MR2
            - $c_{10} = 1.8273 \times 10^6$
            - $c_{01} = -1.7798 \times 10^6$
            - $d = 0.001$
        - MR5
            - $c_{10} = 8.9716 \times 10^5$
            - $c_{01} = -8.2634 \times 10^5$
            - $c_{20} = 8.4566 \times 10^8$
            - $c_{11} = -1.7346 \times 10^9$
            - $c_{02} = 8.893 \times 10^8$
            - $d = 0.001$

- Boundary Conditions

Fixed Boundary conditions applied at the inlet and outlet

Fluid Structure Interface applied to the inner wall of the arteries to enable data transfer between fluid forces and structural deformations

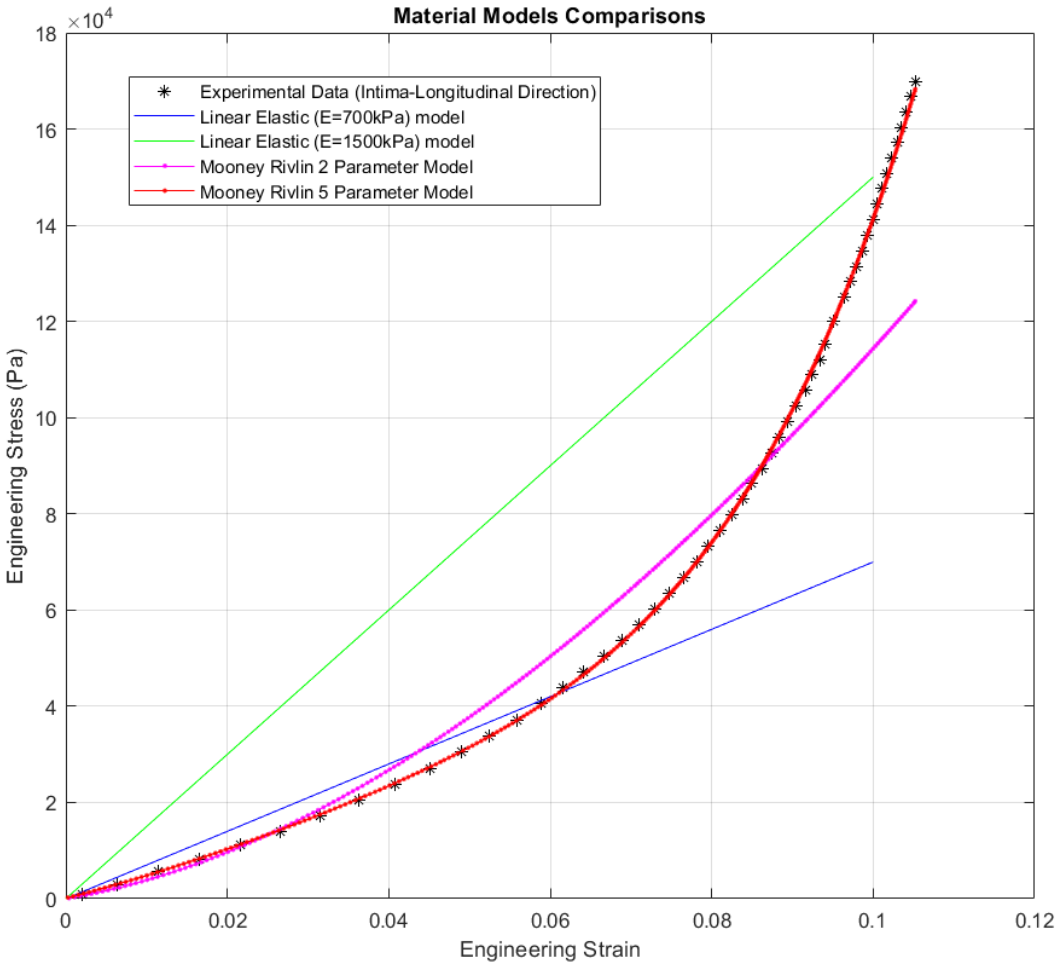

Figure 6: Material Model Comparision Graph

4.2 Implementation

ANSYS was employed to implement the biomechanical model using the workflow shown in the figure below. The model was running using supercomputing resources Katana, using 10 CPUs (2 for mechanical solver and 8 for the fluid solver CFX)

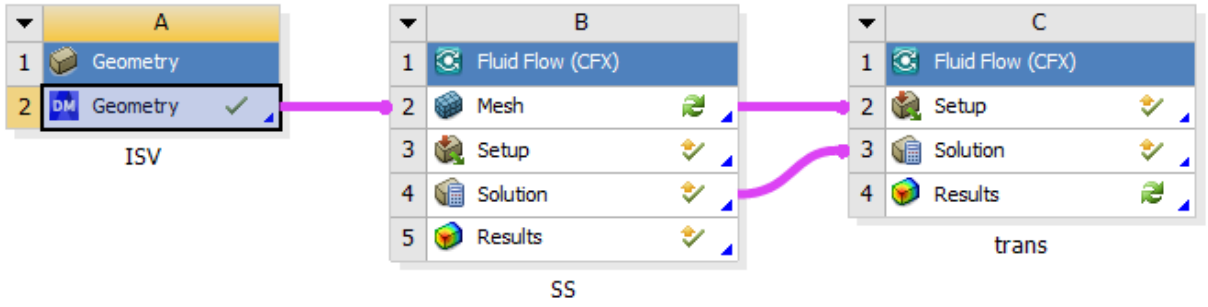

Figure 7: Rigid Wall Simulation Workflow Setup

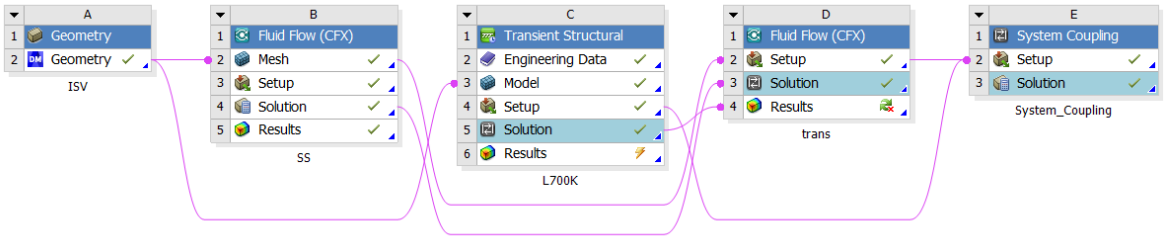

Figure 8: FSI Simulation Workflow Setup

4.3 Workflow Development and Barriers

Major workflow barriers included:

- Obtaining access to the computational resources required for running these simulations
- Developing a functioning FSI simulation using linear elastic material model
- Attempting to adapt the FSI simlulation workflow using linear elastic material to work using nonlinear elastic material models, which was not achieved under the time constraints of the project

Table 4:Nonlinear FSI simulation debugging tests

Test	Aim	Change made	Outcome
Test 1: Convert Vessel Material Model from Linear to Nonlinear Elastic	To run simulation with FSI effects using nonlinear elastic material model	Employ Working Linear Elastic FSI model workflow but using MR2 for vessel wall material properties	Failed due to convergence error
Test 2: Adjust timestep size	To resolve error in Test 1 based on feedback from software error messages	Using the workflow from Test 1 with timestep made smaller	Failed due to convergence error
Test 3: Adjust data transfer steps the steps involved between fluid and structural solver data transfer	To resolve error in Test 1	Using the workflow from Test 1 Increase Data transfer steps from 0 -5 to 5-10 and then 10-20	Delayed failure due to convergence error
Test 4: Adjust fluid material model from Non-Newtonian to Newtonian	To resolve error in Test 3 by employing mimicking setup from literature	Changed the fluid material model to Newtonian	Failed due to convergence error
Test 5: Same as Test 4 with altered structural material compressibility	To resolve error in Test 3 based on expert feedback	Changed the incompressibility parameter for the MR2 model from 0 to 0.1	Increased Delayed failure due to convergence error
Test 6: Alternate Structural solver settings	To resolve errors in Test 5 based on feedback from software error messages	Changed structural solver to employ iterative solver	Same outcome as Test 5
Test 7: Changed vessel material model MR2 to an alternate nonlinear elastic material model	To resolve errors in Test 6 based on expert feedback	Changed nonlinear elastic material model employed for the vessel from MR2 to Neo-Hookean and Ogden model	Failed due to convergence error
Test 8: Change vessel mesh from using solid to shell elements	To resolve errors in Test 6 based on expert feedback	Changed the geometric model to that of a surface with shell elements employed by the structural mesh to simulate wall thickness	Initially worked but when workflow repeated then due to unknown error/changes this failed due to convergence errors

5. Results and discussion

5.1Material Models

5.1.1 WSS Comparison

Impact of Including Fluid Structure Interaction Effect on WSS:

WSS was found to decrease when including FSI interaction effects with a smallest decrease noted with using the L1500k model with its material response being more similar to that of rigid wall model than the L700k model (shown in the figures below)

The significance of these findings may need to be assessed based on the context of WSS data use. In situation such that employed in stent optimsation research [10] this difference could be considered neglible.

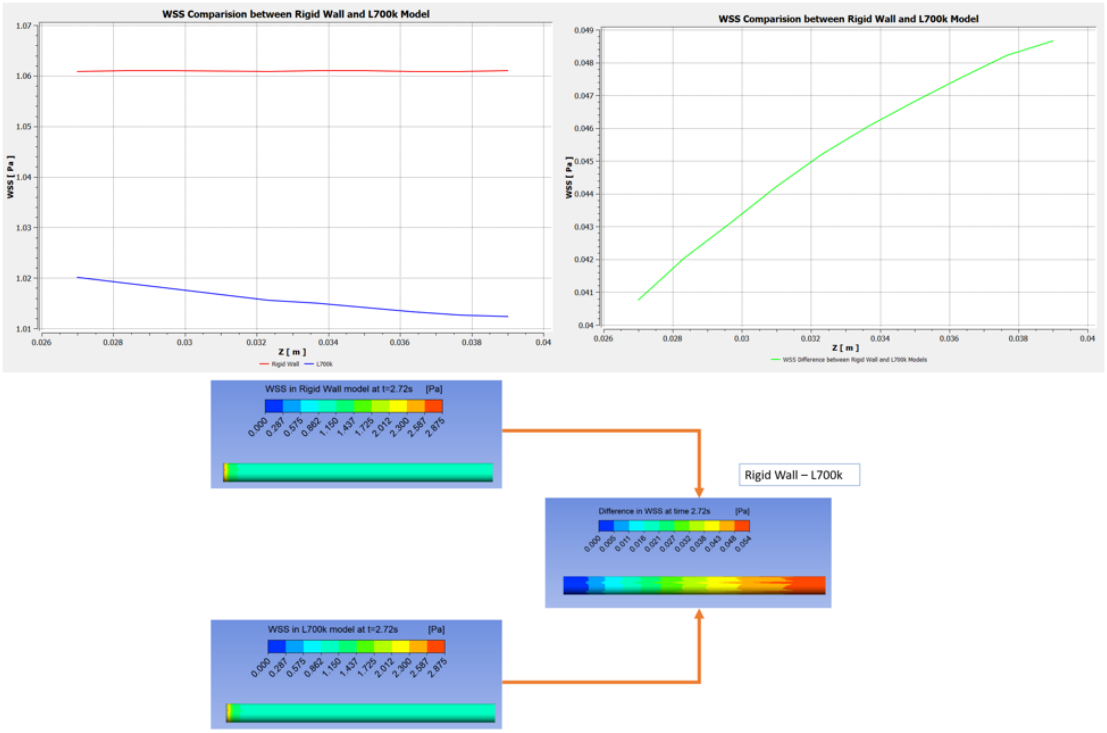

Figure 9: Comparison between Rigid Wall vs L700k model shown as contour plot(below), and as a graph depicting WSS in the ROI(top left) and the difference in WSS between model in the ROI(top right)

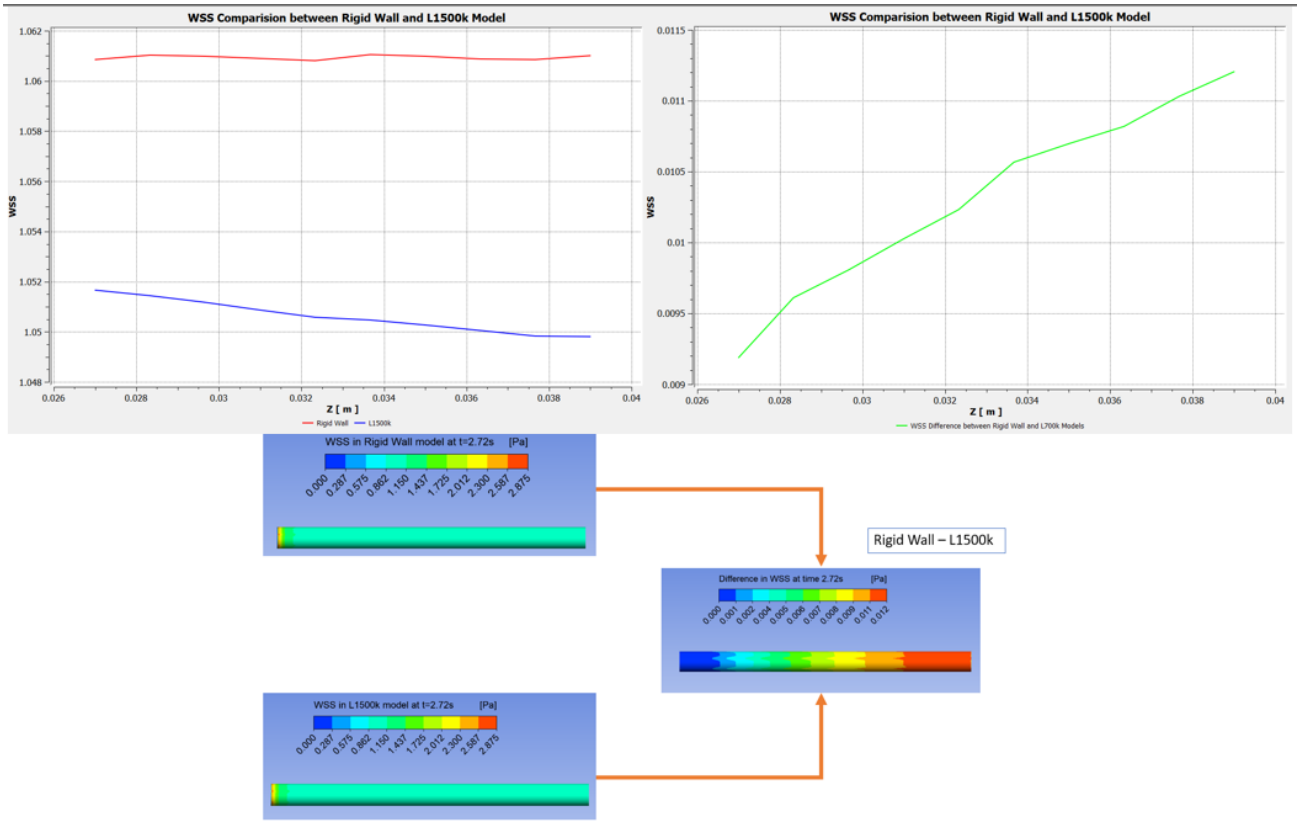

Figure 10:Comparison between Rigid Wall vs L1500k model shown as contour plot(below), and as a graph depicting WSS in the ROI(top left) and the difference in WSS between model in the ROI(top right)

Impact of Varying Linear Elastic Material Stiffness:

A progressive increase in difference between WSS measurements was noted when comparing the model employing the model with ‘low stiffness” behaviour (L700k model) and “high stiffness” behaviour (L1500k model).

The quantiative difference (shown in the figure below) indicates that observed difference may not be meaningful in the context of WSS measurement for conducting threshold analysis as the largest different notes was 0.042 Pa which would be less likely lead to a meaningful difference in threshold analysis results and thus the findings from such research[10], [32].

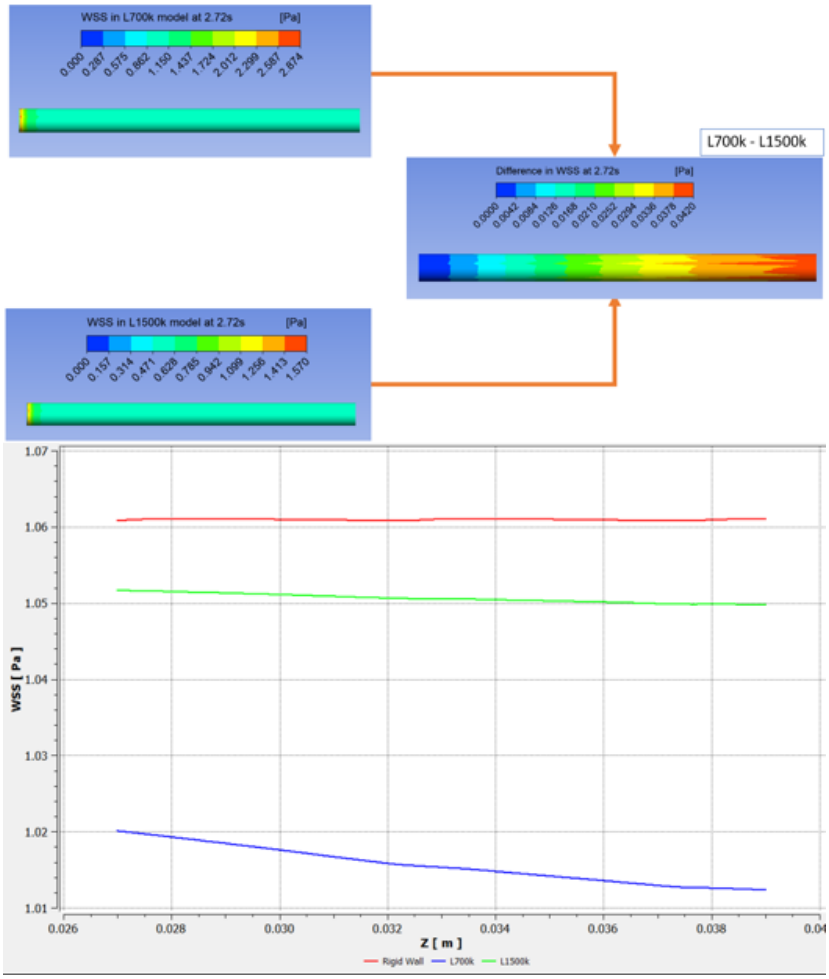

Figure 11: Comparison of WSS contour plots between L700k and 1500k models(above) and WSS between 3 models within ROI

5.1.2 TAWSS Comparison

Impact of Including Fluid Structure Interaction Effect on TAWSS:

Inclusion of FSI effects lead to an increase in TAWSS measurements(shown in the figures below)
But this difference was considered insignificant.in the context of common research appplications[10], [12], [19]

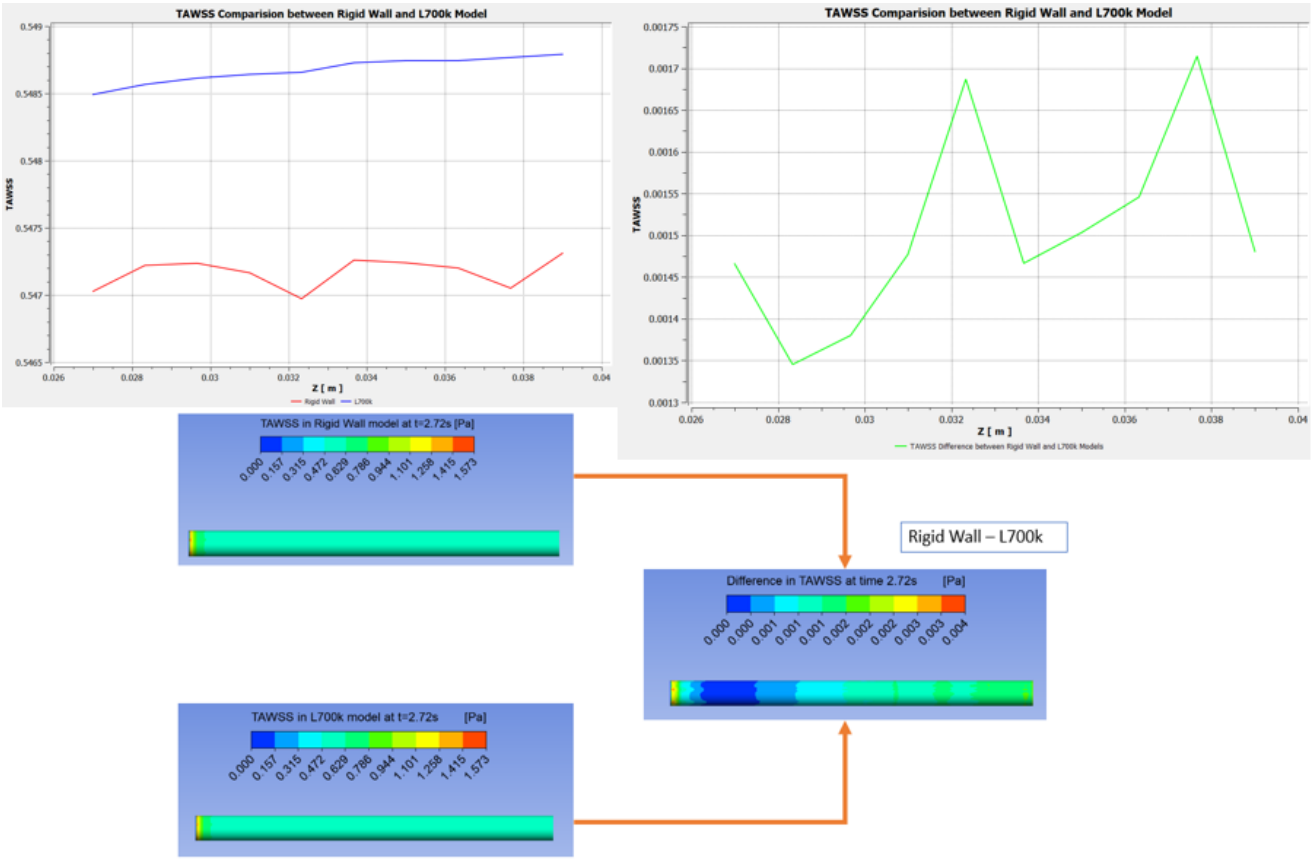

Figure 12: Comparison between Rigid Wall vs L700k model shown as contour plot(below), and as a graph depicting TAWSS in the ROI(top left) and the difference in TAWSS between model in the ROI(top right)

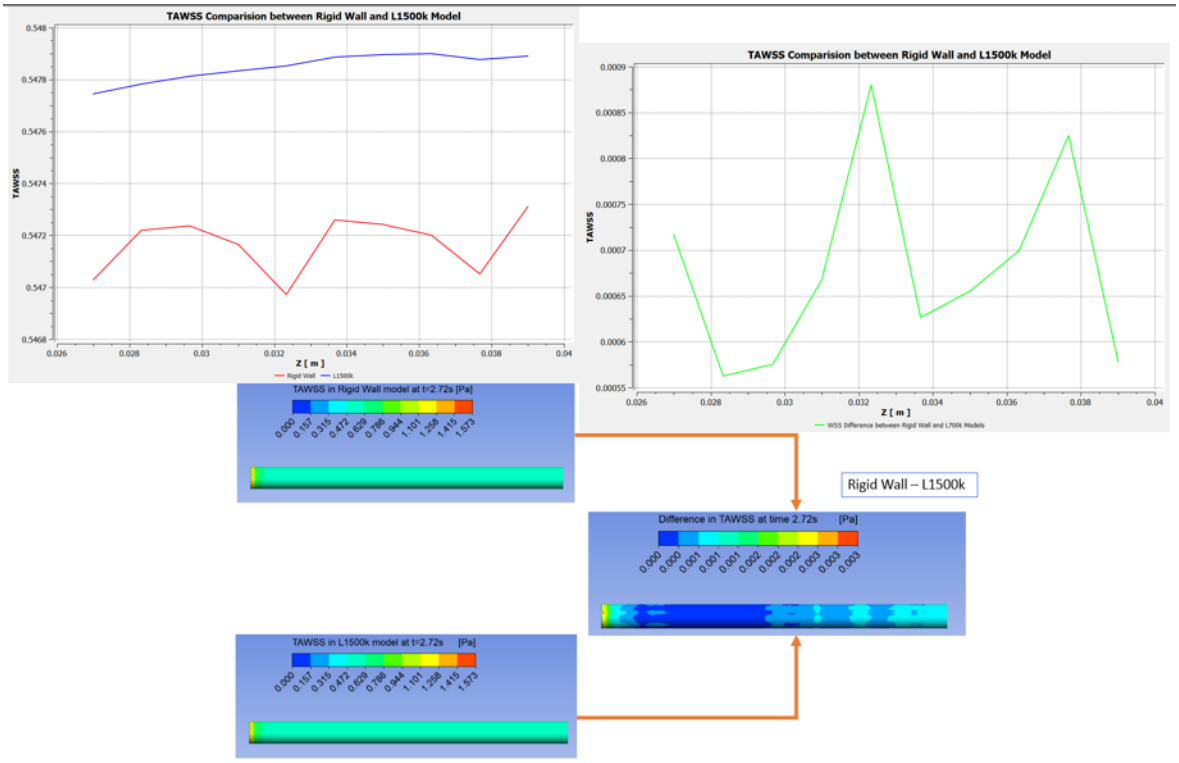

Figure 13: Comparison between Rigid Wall vs L1500k model shown as contour plot(below), and as a graph depicting TAWSS in the ROI(top left) and the difference in TAWSS between model in the ROI(top right)

Impact of Varying Linear Elastic Material Stiffness on TAWSS:

An erractly increase in the difference in TAWSS measurements was observed (shown in the figure below) but as the largest difference is 0.0013Pa, it is proposed that the difference would not have a significant on impact TAWSS measurements.

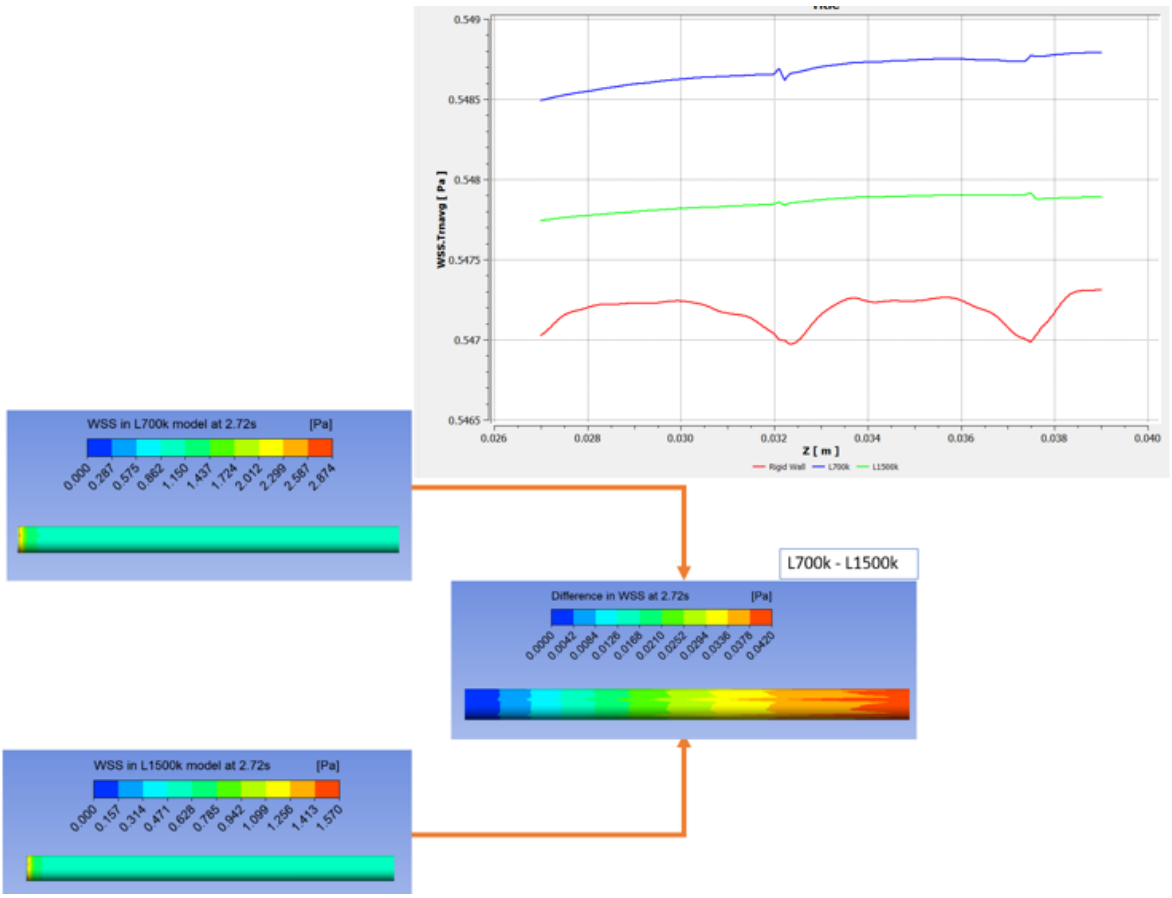

Figure 14:TAWSS Comparision between L700k and 1500k models

5.1.3 Solving Time Comparison

To estimate the costs associated with including interaction effects in biomechanical models for WSS and TAWSS measurements, solving time amongst the 3 models was compared with results shown below

Vessel Wall Material Model	Simulation Time
Rigid Wall Model	684s ≈ 11mins
L700k	6585s ≈ 109mins
L1500k	6574 ≈ 109mins

Wall Material Model Comparisons	Simulation Time Difference & Percentage Difference
L700k vs Rigid Wall	5901s ≈ 862 % increase
L1500k vs Rigid Wall	5890s ≈ 861% increase
L1500k vs L700k	-11s ≈ -0.2% decrease

Figure 15: Solving Time Comparision

An 8-fold increase in solving was noted between the FSI models and the Rigid Wall model, with these being similar to those noted in the literature[25].

This difference could represent a meaningful data point against including FSI simulation in the context of research optimizing stent designs using just WSS and TAWSS, as the multiple simulations required for these studies as well as the increased costs with FSI models could lead to significant research delay with minimal difference in final outcomes.

5.1.4 Verification and Validation

In the absence of experimental in vivo data, it can be difficult to assess the validatity of the data but mesh verification using the Rigid Wall model was conducted to ensure the fluid mesh would be sufficient to reduce noise in WSS and TAWSS data associated with numerical errors. The fluid mesh with close to 200K elements was employed for all models.

Table 5: Mesh Verifcation Test

MESH (ELEMENT NUMBER)	Difference in Average TAWSS (Pa)	Percentage Difference in Average TAWSS
41K	0.557568	1.29
110K	0.562035	0.51
207k	**0.564458**	**0.08**

5.2 Limitations and Future Recommendations

Limitations

- Data might be influned by numerical errors in solid mesh grid convergence should be conducted.
- Geometric Model Approximation may influence these findings should be verified using more realistic arterial geometry models of the vessel and its wall.
- Material Model choices were not completely explored in this project with data not obtained when including FSI effects using nonlinear elastic material model due to simulation setup errors. It is suggested that an alternate solver employed in literature[25] that employ explicit dynamics solver should be considered as an option to potentially avoid convergence errors encountered in current project.

Future Work

- Validation with Experimental Model using compliant vessel models.
- Replicate workflow using more models of artery geometry to verify stability of findings.
- Adapt current workflow to be allow WSS and TAWSS data collection using nonlinear elastic vessel wall material model
- Assess if current findings are applied to a stent optimization workflow and/or disease prediction workflow, this may lead to major change in results when data collected using simulations without including FSI effects.

6 Conclusions

Improvements in measurements of biomechanical data could facilitate improved decisions making in research associated with the management and treatment of CAD, incorporating FSI interactions effects to obtain more realistic WSS data was found to lead to increase in WSS values and solving time and decrease in TAWSS but the difference in TAWSS and WSS data was considered insignificant in the context of current usage WSS and TAWSS in the literature with changes in material stiffness having minimal influence of the size of the difference but more future data may be needed using nonlinear elastic material models and patient bifurcated geometries to clarify the utility of including FSI effects when measuring biomechanical data.

References

[1] L. Zhong, J.-M. Zhang, B. Su, R. S. Tan, J. C. Allen, and G. S. Kassab, 'Application of Patient-Specific Computational Fluid Dynamics in Coronary and Intra-Cardiac Flow Simulations: Challenges and Opportunities', *Frontiers in Physiology*, vol. 9, Jun. 2018, doi: 10.3389/fphys.2018.00742.
[2] F. Sanchis-Gomar, C. Perez-Quilis, R. Leischik, and A. Lucia, 'Epidemiology of coronary heart disease and acute coronary syndrome', *Annals of Translational Medicine*, vol. 4, no. 13, pp. 256–256, Jul. 2016, doi: 10.21037/atm.2016.06.33.
[3] J. Wang *et al.*, 'Endovascular stent-induced alterations in host artery mechanical environments and their roles in stent restenosis and late thrombosis', *Regenerative Biomaterials*, vol. 5, no. 3, pp. 177–187, Jun. 2018, doi: 10.1093/rb/rby006.
[4] A. J. Brown, Z. Teng, P. C. Evans, J. H. Gillard, H. Samady, and M. R. Bennett, 'Role of biomechanical forces in the natural history of coronary atherosclerosis', *Nature Reviews Cardiology*, vol. 13, no. 4, pp. 210–220, Apr. 2016, doi: 10.1038/nrcardio.2015.203.
[5] L. D. C. Casa, D. H. Deaton, and D. N. Ku, 'Role of high shear rate in thrombosis', *Journal of Vascular Surgery*, vol. 61, no. 4, pp. 1068–1080, Apr. 2015, doi: 10.1016/j.jvs.2014.12.050.
[6] K. K. L. Wong, D. Wang, J. K. L. Ko, J. Mazumdar, T.-T. Le, and D. Ghista, 'Computational medical imaging and hemodynamics framework for functional analysis and assessment of cardiovascular structures', *BioMedical Engineering OnLine*, vol. 16, no. 1, Dec. 2017, doi: 10.1186/s12938-017-0326-y.
[7] 'Coronary Arteries: How It Works & Images', *Cleveland Clinic*. https://my.clevelandclinic.org/health/articles/17063-coronary-arteries (accessed May 09, 2020).
[8] 'Atherosclerosis', *Wikipedia*. May 05, 2020, Accessed: May 09, 2020. [Online]. Available: https://en.wikipedia.org/w/index.php?title=Atherosclerosis&oldid=955032161.
[9] J. M. Tarbell, Z.-D. Shi, J. Dunn, and H. Jo, 'Fluid Mechanics, Arterial Disease, and Gene Expression', *Annual Review of Fluid Mechanics*, vol. 46, no. 1, pp. 591–614, Jan. 2014, doi: 10.1146/annurev-fluid-010313-141309.
[10] S. Beier *et al.*, 'Hemodynamics in Idealized Stented Coronary Arteries: Important Stent Design Considerations', *Annals of Biomedical Engineering*, vol. 44, no. 2, pp. 315–329, Feb. 2016, doi: 10.1007/s10439-015-1387-3.
[11] J. Ormiston *et al.*, 'Bench testing and coronary artery bifurcations: a consensus document from the European Bifurcation Club', *EuroIntervention*, vol. 13, no. 15, pp. e1794–e1803, Feb. 2018, doi: 10.4244/EIJ-D-17-00270.
[12] F. Gijsen *et al.*, 'Expert recommendations on the assessment of wall shear stress in human coronary arteries: existing methodologies, technical considerations, and clinical applications', *European Heart Journal*, vol. 40, no. 41, pp. 3421–3433, Nov. 2019, doi: 10.1093/eurheartj/ehz551.
[13] B. Owen, N. Bojdo, A. Jivkov, B. Keavney, and A. Revell, 'Structural modelling of the cardiovascular system', *Biomechanics and Modeling in Mechanobiology*, vol. 17, no. 5, pp. 1217–1242, Oct. 2018, doi: 10.1007/s10237-018-1024-9.
[14] D. Bluestein, 'Utilizing Computational Fluid Dynamics in Cardiovascular Engineering and Medicine-What You Need to Know. Its Translation to the Clinic/Bedside: Invited Editorial', *Artificial Organs*, vol. 41, no. 2, pp. 117–121, Feb. 2017, doi: 10.1111/aor.12914.
[15] Z. Sun and L. Xu, 'Computational fluid dynamics in coronary artery disease', *Computerized Medical Imaging and Graphics*, vol. 38, no. 8, pp. 651–663, Dec. 2014, doi: 10.1016/j.compmedimag.2014.09.002.
[16] S. Beier *et al.*, 'Impact of bifurcation angle and other anatomical characteristics on blood flow – A computational study of non-stented and stented coronary arteries', *Journal of Biomechanics*, vol. 49, no. 9, pp. 1570–1582, Jun. 2016, doi: 10.1016/j.jbiomech.2016.03.038.
[17] V. Thondapu *et al.*, 'Endothelial shear stress 5 years after implantation of a coronary bioresorbable scaffold', *European Heart Journal*, vol. 39, no. 18, pp. 1602–1609, May 2018, doi: 10.1093/eurheartj/ehx810.

[18] K.-S. Han *et al.*, 'Direct Assessment of Wall Shear Stress by Signal Intensity Gradient from Time-of-Flight Magnetic Resonance Angiography', *BioMed Research International*, vol. 2017, pp. 1–8, 2017, doi: 10.1155/2017/7087086.
[19] F. Rikhtegar *et al.*, 'Choosing the optimal wall shear parameter for the prediction of plaque location—A patient-specific computational study in human left coronary arteries', *Atherosclerosis*, vol. 221, no. 2, pp. 432–437, Apr. 2012, doi: 10.1016/j.atherosclerosis.2012.01.018.
[20] J. S. Tran, D. E. Schiavazzi, A. B. Ramachandra, A. M. Kahn, and A. L. Marsden, 'Automated tuning for parameter identification and uncertainty quantification in multi-scale coronary simulations', *Computers & Fluids*, vol. 142, pp. 128–138, Jan. 2017, doi: 10.1016/j.compfluid.2016.05.015.
[21] R. A. Macrae, K. Miller, and B. J. Doyle, 'Methods in Mechanical Testing of Arterial Tissue: A Review: Methods in Mechanical Testing of Arterial Tissue: A Review', *Strain*, vol. 52, no. 5, pp. 380–399, Oct. 2016, doi: 10.1111/str.12183.
[22] G. A. Holzapfel, G. Sommer, C. T. Gasser, and P. Regitnig, 'Determination of layer-specific mechanical properties of human coronary arteries with nonatherosclerotic intimal thickening and related constitutive modeling', *American Journal of Physiology-Heart and Circulatory Physiology*, vol. 289, no. 5, pp. H2048–H2058, Nov. 2005, doi: 10.1152/ajpheart.00934.2004.
[23] P. Eslami *et al.*, 'Effect of Wall Elasticity on Hemodynamics and Wall Shear Stress in Patient-Specific Simulations in the Coronary Arteries', *Journal of Biomechanical Engineering*, vol. 142, no. 2, Feb. 2020, doi: 10.1115/1.4043722.
[24] J. Dong, Z. Sun, K. Inthavong, and J. Tu, 'Fluid–structure interaction analysis of the left coronary artery with variable angulation', *Computer Methods in Biomechanics and Biomedical Engineering*, vol. 18, no. 14, pp. 1500–1508, Oct. 2015, doi: 10.1080/10255842.2014.921682.
[25] C. Chiastra, F. Migliavacca, M. Á. Martínez, and M. Malvè, 'On the necessity of modelling fluid–structure interaction for stented coronary arteries', *Journal of the Mechanical Behavior of Biomedical Materials*, vol. 34, pp. 217–230, Jun. 2014, doi: 10.1016/j.jmbbm.2014.02.009.
[26] P. D. Morris *et al.*, 'Computational fluid dynamics modelling in cardiovascular medicine', *Heart*, vol. 102, no. 1, pp. 18–28, Jan. 2016, doi: 10.1136/heartjnl-2015-308044.
[27] M. Malvè, A. García, J. Ohayon, and M. A. Martínez, 'Unsteady blood flow and mass transfer of a human left coronary artery bifurcation: FSI vs. CFD', *International Communications in Heat and Mass Transfer*, vol. 39, no. 6, pp. 745–751, Jul. 2012, doi: 10.1016/j.icheatmasstransfer.2012.04.009.
[28] D. Meza, D. A. Rubenstein, and W. Yin, 'A Fluid–Structure Interaction Model of the Left Coronary Artery', *Journal of Biomechanical Engineering*, vol. 140, no. 12, p. 121006, Sep. 2018, doi: 10.1115/1.4040776.
[29] L. Wang *et al.*, 'Fluid-structure interaction models based on patient-specific IVUS at baseline and follow-up for prediction of coronary plaque progression by morphological and biomechanical factors: A preliminary study', *Journal of Biomechanics*, vol. 68, pp. 43–50, Feb. 2018, doi: 10.1016/j.jbiomech.2017.12.007.
[30] J. Wu, G. Liu, W. Huang, D. N. Ghista, and K. K. L. Wong, 'Transient blood flow in elastic coronary arteries with varying degrees of stenosis and dilatations: CFD modelling and parametric study', *Computer Methods in Biomechanics and Biomedical Engineering*, vol. 18, no. 16, pp. 1835–1845, Dec. 2015, doi: 10.1080/10255842.2014.976812.
[31] J. Wang *et al.*, 'Optical coherence tomography-based patient-specific coronary artery reconstruction and fluid–structure interaction simulation', *Biomechanics and Modeling in Mechanobiology*, vol. 19, no. 1, pp. 7–20, Feb. 2020, doi: 10.1007/s10237-019-01191-9.
[32] G. Alaimo, F. Auricchio, M. Conti, and M. Zingales, 'Multi-objective optimization of nitinol stent design', *Medical Engineering & Physics*, vol. 47, pp. 13–24, Sep. 2017, doi: 10.1016/j.medengphy.2017.06.026.